*internal report* **257**

# Effect of seasonal vegetation on hydrology and erosion at Ranger uranium mine

Elizabeth George
Garry Willgoose

May 1997

*supervising scientist*

# EFFECT OF SEASONAL VEGETATION ON HYDROLOGY AND EROSION AT RANGER URANIUM MINE

by

**Elizabeth George and Garry R Willgoose**

**Department of Civil, Surveying and Environmental Engineering,**
**University of Newcastle,**
**NSW Australia.**

May 1997

JR-05-181

eriss

ENVIRONMENTAL RESEARCH INSTITUTE OF THE SUPERVISING SCIENTIST

# ABSTRACT

This project is part of ongoing research at Ranger Uranium Mine to ensure that there will be no contaminants released from the mine site into the surrounding Kakadu National Park within a design life of 200 years.

A soil site and a number of ripped plots situated on the Waste Rock Dump at Ranger Uranium Mine, in the Northern Territory, are analysed in this report in order to determine the effect vegetation growth has on the erosion and hydrology characteristics of waste rock. Monitoring was carried out on the Soil Site during the 95/96 Wet season.

Storms monitored on the soil site, and 1993 rainfall simulations on the ripped plots were used to calibrate the kinematic wave model DISTFW NLFIT.

Data directly observed from the soil site indicates that the effect of vegetation on the hydrology of the soil does not vary significantly between the beginning and end of the 95/96 Wet Season.

The soil site does have high infiltration rates, but whether the high infiltration rates are due to the vegetation was not able to be determined. There is not a constant increase in infiltration over the wet season.

Erosion results indicate that vegetation growth over the wet season may decrease the erosion off the soil site.

# TABLE OF CONTENTS

# List of Figures

# List of Tables

# ABBREVIATIONS

| | |
|---|---|
| $A_r$ | total flow area of catchment [$m^2$] |
| $\beta$ | coefficient of sediment transport equation |
| $c_g$ | coefficient on the groundwater storage equation [$sm^{-1}$] |
| $c_r$ | coefficient on the kinematic wave equation [$m^{(3-2e_m)}\ s^{-1}$] |
| $c_s$ | coefficient on the surface storage equation [$m^{(1-2\gamma)}\ s^{\gamma}$] |
| DISTFW NLFIT | Distributed Field Williams Non-Linear Fit Model |
| $e_m$ | exponent on the kinematic wave equation |
| ERA | Energy Resources of Australia Ltd |
| ***eriss*** | Environmental Research Institute of the Supervising Scientist |
| f | infiltration capacity rate [m/s] |
| $\gamma$ | exponent on the surface storage equation |
| $\phi$ | long - term steady state infiltration rate [m/s] |
| K | conveyance [$m^3/s$] |
| m | exponent of sediment transport equation |
| n | exponent of sediment transport equation |
| q | discharge per unit width [$l.s^{-1}.m^{-1}$ ] |
| $q_s$ | sediment discharge per unit width [g. $s^{-1}$. $m^{-1}$ ] |
| RUM | Ranger Uranium Mine |
| S | local slope [m/m] |
| $S_\phi$ | sorptivity (in the Philip infiltration equation) [$ms^{-1/2}$] |
| t | time [s] |
| WRD | Waste Rock Dump |

# 1. INTRODUCTION

## 1.1 General

Ranger Uranium Mine (RUM) is located approximately 260 km east of Darwin, Northern Territory. Ranger Uranium Mine is owned and operated by Energy Resources of Australia Ltd (ERA) and operates on a 78 $km^2$ lease which is not part of Kakadu National Park. Figure 1 shows a map of RUM.

The development of the Ranger uranium deposits at Jabiru, Northern Territory, was proposed by the then Australian Atomic Energy Commission and Ranger Uranium Mines Pty Ltd. In response to this proposal, the Australian Commonwealth Government established the Ranger Uranium Environmental Inquiry in April 1975 under the *Environmental Protection (Impact of Proposals) Act.*

In 1977, the Government announced its decision to authorise the mining and export of uranium under very strict requirements for environmental control recommended by the Ranger Uranium Environmental Inquiry. The requirements included the establishment of Kakadu National Park and the establishment of a Supervising Scientist, now the Environmental Research Institute of the Supervising Scientist (***eriss***). The role of the Supervising Scientist was to carry out research on the impact of uranium mining on the environment, assist in development of measures for the protection of the environment, and oversee their implementation.

Commonwealth Government regulations require that radioactive mill tailings and other contaminants do not escape from the containment landform into the surrounding National Park within a design life of 200 years (Commonwealth of Australia, 1987).

In the Top End of the Northern Territory there are two distinctive seasons, the 'wet' and the 'dry'. The wet season is the hot, humid period from October to April. Most of the rain falls between December to March, a period of high humidity and torrential rain, which occurs under the influence of north west monsoon winds. The dry season is the period from May to September, where very little rain falls. The average rainfall for June is 2 mm, which contrasts with the average rainfall for January of 338 mm. The average annual rainfall is around 1500 mm.

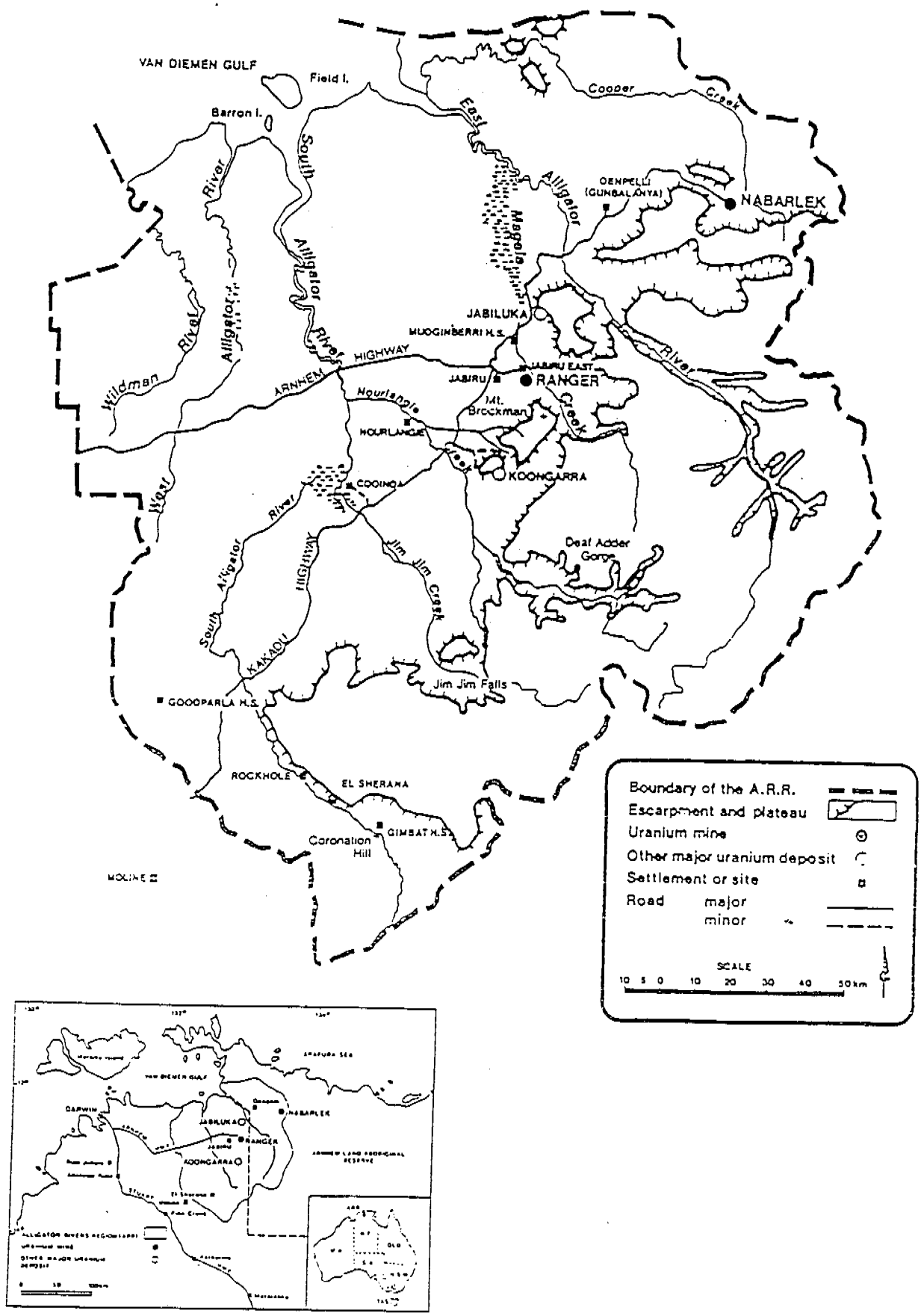


Figure 1. Locality of the Ranger Uranium Mine (Supervising Scientist, 1985).

## 1.2 Objectives

The project involves hydrologic, sediment transport, and vegetation studies at the soil site on the Waste Rock Dump (WRD) at Ranger Uranium Mine. Hydrologic studies were also carried out for 1993 rainfall simulations at the ripped plots on the WRD.

The aims of this project are to determine:

1. The effect vegetation growth has on the hydrology of the soil site as the wet season proceeds,
2. Whether vegetation causes a seasonal effect on infiltration and if there is a constant increase in infiltration over the wet season,
3. The effect of vegetation growth on the erosion of the soil site,
4. The effect of ripping (analysis of the 1993 ripped plots data); and
5. The combined effect of ripping and vegetation on the hydrology of the soil site.

# 2. METHODOLOGY

## 2.1 Outline of Sites Used

### 2.1.1 Soil Site

The soil site was monitored to determine whether the rate of vegetation growth throughout the wet season has an effect on the hydrology of the site.

The soil site, situated on the WRD, RUM was constructed in November 1994 as described in Saynor, Evans, Smith and Willgoose (1995).

The soil site has an average slope of 0.012m/m and was constructed on a surface ripped, top-soiled and revegetated area of the upper surface of the northern part of the WRD. The soil site is 30.0m long by 20.0m wide (600m$^2$). A topographic survey had previously been conducted of the soil site. The site is vegetated with small acacias, grasses (predominantly spear grass) and other species. Before the onset of the 95-96 wet season the soil site was stripped of vegetation. I observed that during the first month of the wet season, the spear grass grew extremely fast, up to 15 centimetres in one week.

Figure 2 is a contour map of the soil site, created by ***eriss*** staff.

A preliminary assessment of the effect of vegetation on the long term erosional stability of Ranger has been carried out by Garry Willgoose. The assessment predicted the erosion rate of a fully developed vegetated undergrowth and canopy to be approximately 5.8% of unvegetated erosion.

### 2.1.2 Ripped Plots

To assist revegetation and erosion control, waste rock dumps will undergo some form of surface preparation. One option is surface ripping. To study optimum ripping strategies, six plots with various ripping patterns were established on the RUM WRD. The six different ripping patterns are described in Table 1 below, and are shown in Figure 3.

Table 1 - Ripping patterns

| Plot | Ripping pattern |
|---|---|
| 1 | Diagonal cross ripping, 3 m spacing, 1 m deep |
| 2 | Rectangular cross ripping, 3 m spacing, 0.5 m deep |
| 3 | Linear pattern across the slope, 2 m spacing, 0.5 m deep |
| 4 | Linear pattern across the slope, 3 m spacing, 1 m deep |
| 5 | Linear pattern across the slope, 2 m spacing, 1 m deep |
| 6 | Rectangular cross ripping, 3 m spacing, 1 m deep |

Rainfall simulation studies were conducted on these plots in 1991 and hydrology data collected. Finnegan (1993) used data obtained to:

1. calibrate the Field Williams rainfall-runoff model to determine kinematic and infiltration properties for the ripping treatment, and

2. statistically assess the difference between the different ripping strategies.

Finnegan (1993) found that, "..the steady infiltration rates calculated by the model indicated that all ripping treatments increased the infiltration capacity rate of the spoil dumps as compared with infiltration rates calculated in previous studies of unripped surfaces." The study concluded that an accurate assessment of the model's runoff-routing parameters could not be made due to incomplete knowledge of temporal fluctuations in the spatial distribution of rainfall. This prevented the predicted discharge accurately fitting the observed discharge in the DISTFW model. Finnegan (1993) was unable to determine whether significant differences existed between the hydrologic parameters associated with the six ripping treatments.

In 1993, rainfall simulation experiments were again conducted on the ripped plots to assess the temporal effects of weathering and settlement on the hydrology of the ripped surfaces. Erosion and hydrology data were collected during the simulations and were reduced by ***eriss*** staff. The data obtained from the 1993 rainfall simulations on the ripped plots were analysed in this report.

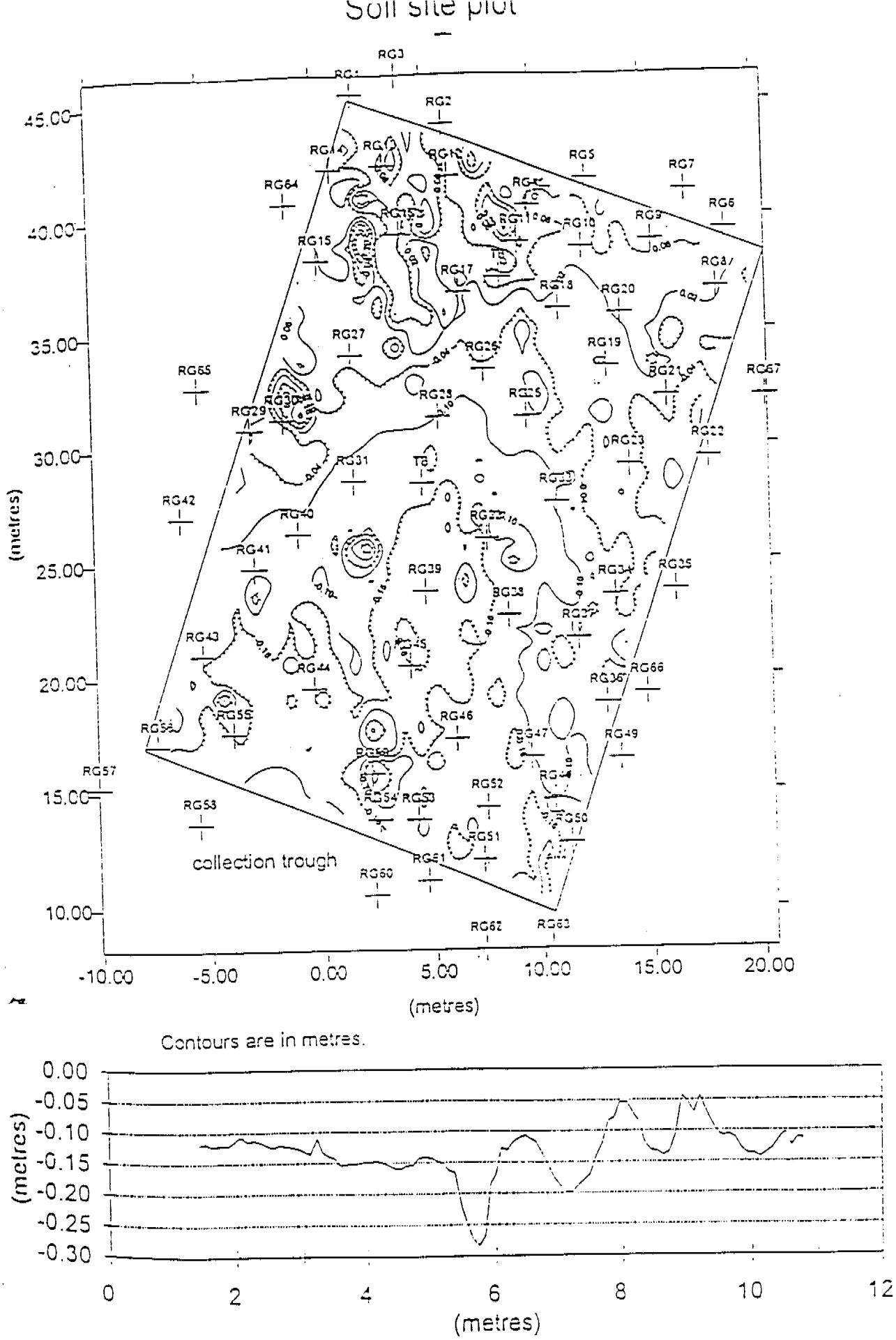


Figure 2 Topographic contour map of the soil site, and 10 m cross section (not to scale) at 100mm intervals (below).

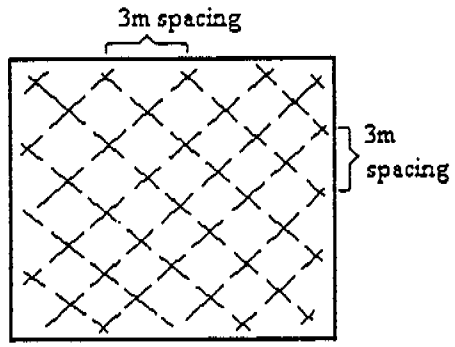


**Ripped plot 1.** 1m deep

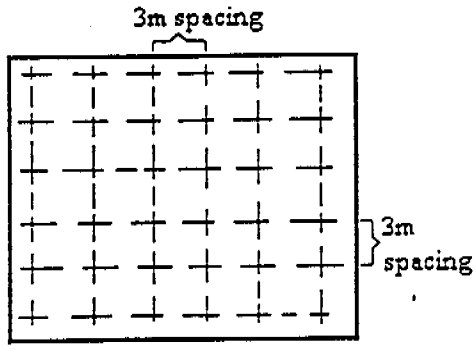


**Ripped plot 2.** 0.5m deep

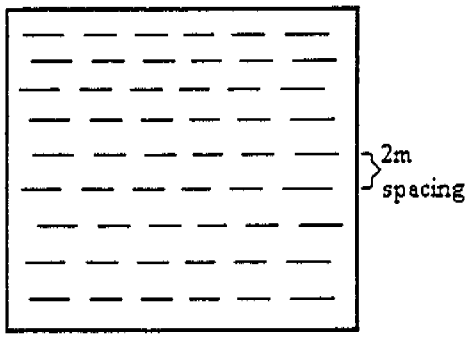


**Ripped plot 3.** 0.5m deep

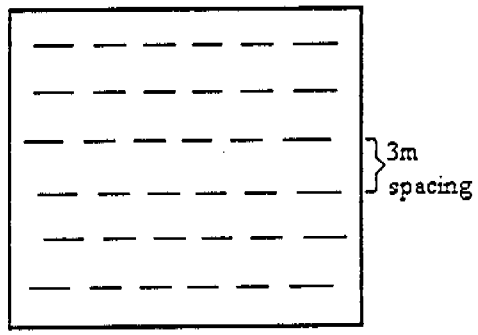


**Ripped plot 4.** 1m deep

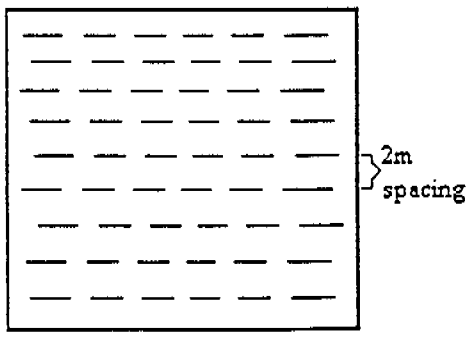


**Ripped plot 5.** 1m deep

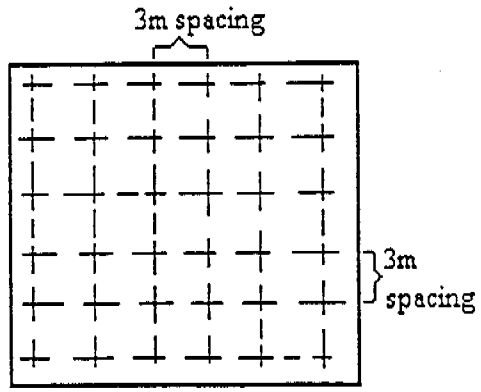


**Ripped plot 6.** 1m deep

Figure 3. Ripping patterns and plot numbers for the ripped plots. In all cases the downslope direction is down the page.

## 2.2 Data Collection Procedure

### 2.2.1 Soil Site Data Collection

To achieve the objectives of the project, I undertook the following tasks during the 95/96 wet season:

1. Data collection of daily rainfall and collection of bedload from the soil site for storms greater than 10 mm,
2. Monitoring of storms to collect sediment and discharge data, and
3. Vegetation survey of the soil site.

#### 2.2.1.1 Hydrology

- **Monitoring rainfall on a daily basis**

I monitored natural rainfall events on the WRD at the soil site between 11/12/95 and 16/2/96 using the methods described in Saynor *et al* (1995). The cumulative rainfall was measured using a 0.2 mm tipping bucket raingauge placed in the centre of the site. The spear grass grew up to 1 metre tall around the raingauge by the end of the wet season. This did not affect the amount of rainfall recorded by the raingauge as the rain falls perpendicular to the site (not on an angle).

During a rainfall event, water and bedload (soil) flows into a trough at the base of the site, into a stilling basin, and then through a flume. The stage in the flume was logged using a capacitance rod.

Both the raingauge and the capacitance rod data were recorded on a DATATAKER D50 datalogger sampling at 30 second intervals. The data were downloaded to a Toshiba T1910 portable computer daily, using a software package called DeTerminal. This allowed hydrology data to be collected for storm events without an observer present.

Photographs of the instruments used are shown on the following pages.

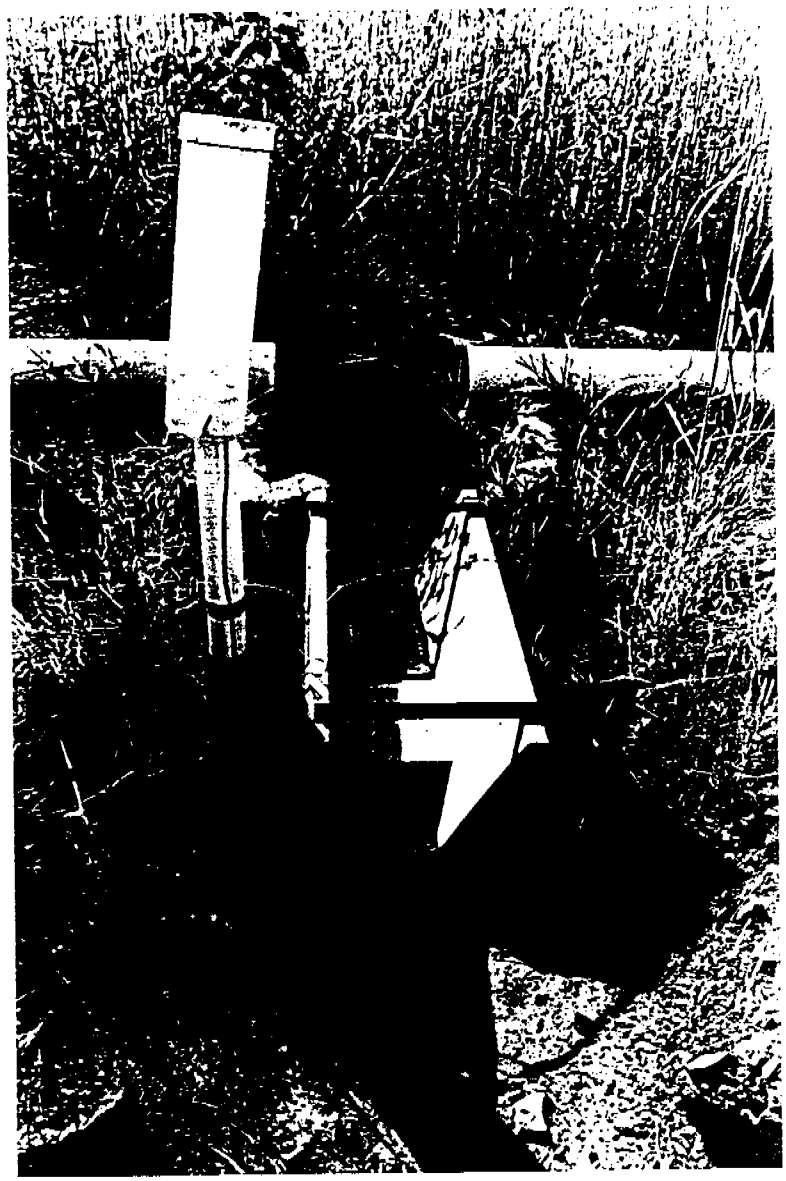

Capacitance Rod and Flume

Tipping Bucket Raingauge at end of 95/96 Wet Season

Datalogger and Laptop

- **Monitoring storms at the soil site**

Rainfall events were also monitored with an observer present. Runoff samples were collected from the flume for suspended sediment analysis, and the depth of water discharging over the flume was measured. I monitored storms on 14/12/95 and 10/1/96. There was 14.8 mm recorded at the soil site on 14/12/95, and 88.8 mm recorded on 10/1/96.

## 2.2.1.2 Sediment

- **Bedload sample analysis**

When the rainfall event recorded on the datalogger was greater than 10 mm, I collected the bedload and determined the soil losses in the laboratory. I also collected the bedload from the trough and reservoir at the conclusion of monitored rainfall events (when an observer was present).

The collected bedload was placed in pre-weighed aluminium containers, dried at 105°C and reweighed to obtain the mass of sediment and containers. The container mass was then subtracted from the oven dried mass to give a total bedload mass.

Particle size analysis was carried out by myself on the bedload from the monitored storms (14/12/95 and 10/1/96) and the bedload collected on 8/2/96 at the soil site. This was used to determine whether the distribution of particle sizes change throughout the wet season.

- **Suspended sediment sample analysis**

The suspended load is the material suspended in the flow by the flow turbulence.

For each storm monitored with an observer present, the runoff from the flume was collected in sample bottles approximately every minute. I analysed the samples at the laboratory for conductivity and suspended sediment concentration. After conductivity was measured the samples were transferred into an aluminium tray of known weight and dried in an oven at 105°C. The weight of the tin and sediment were measured and all results were entered into a spreadsheet.

### 2.2.1.3 Vegetation survey of the soil site

The vegetation was surveyed on a weekly basis, by myself, to determine the rate of growth. The vegetation survey consisted of setting out four permanent $1m^2$ quadrats on the soil site. Photographs were taken of each quadrat to calculate the percentage cover. The average grass height was estimated for each quadrat by taking an average of at least 10 random measurements of total grass height (the height of the tallest blade). The percentage cover was estimated, as was the percentage similarity between the sample quadrat and the rest of the plot. Photographs of the four quadrats throughout the 95/96 wet season are contained in Appendix A.

The biomass was sampled using four $0.2m^2$ quadrats with a similar vegetation density to each of the four $1m^2$ quadrats. All vegetation, including the roots were removed and placed in a paper bag of known weight. The samples (in the paper bags) were all placed in an oven at 100°C. The dry weight of the vegetation and the bag was recorded and the dry weight of the biomass calculated. The biomass samples were taken on site. The error produced in any additional erosion off the site would be negligible because less than 1% of the site has been sampled for biomass. Bayesian probability will be used in the data analysis, which is the reason why the percentage similarity between the $1m^2$ quadrats was estimated.

Photographs were taken (4 in total) of the $600m^2$ plot to show the rate of vegetation growth, shown in Appendix A. The same reference point was used to centre the photograph on each date.

## 2.2.2 Ripped Plots Data Collection

All experimental work conducted on the ripped plots were performed by the Erosion and Hydrology Group at ***eriss***.

## 2.3 Data Reduction

### 2.3.1 Survey Data

The soil site had previously been surveyed, and subcatchment boundaries and properties defined (Figure 2).

All ripped plots required subplot boundaries and parameters to be defined. An executable file, survey.exe, was used to convert the raw survey data files (input files) into files containing x, y, z coordinates in columns (output files). The output files were then opened in the SURFER worksheet. I then produced the survey grid in SURFER.

The contour maps I produced for ripped plots 1 to 6 are contained in Appendix B.

### 2.3.2 Calculation of subplot width, length, area, slope and kinematic wave ($C_r$)

The same subcatchment parameters were used for the soil site as in Saynor *et al* (1995).

Each Ripped plot was divided into subplots and the boundary for each subplot was determined from the contour plots (Appendix B). The length, width, and area of each subplot was calculated using the discretize option in SURFER. This gave the x, y coordinates at each corner of the subplot. The length of each subplot was calculated to be the average of the lengths at either side of the subplot. The width of each subplot was assumed to be equal, and was calculated to be the average of all the subplot widths. The area was calculated from the lengths and widths of each subplot. The change in elevation was determined by subtracting the downhill boundary contour from the uphill boundary contour of the subplot. The value of the parameter $C_r$ was calculated from the following equation:

$$C_r = \frac{1}{width^{\frac{2}{3}}}$$

The length, width, area, change in elevation and $C_r$, calculated for each subplot, are contained in Appendix C.

The areas of each subplot were added and compared to the total plot area calculated by the grid volume option in SURFER. They were also compared to the area calculated by Finnegan (1993). The areas of each ripped plot calculated from the 3 different methods are shown in Appendix C.

### 2.3.3 Rainfall data

Rainfall data used for the soil site was that recorded by the tipping bucket raingauge for each natural rainfall event. For the monitored storms, I reduced the data in a similar method to that of Saynor *et al* (1995). The data files were edited and imported into a spreadsheet. The capacitance rod measures the relative difference in depth of water passing over the flume. I selected a capacitance for zero so that the runoff from the site would start at zero. The time recorded for zero flows were compared with the logged times. The capacitance for zero flow was selected to be the capacitance for zero head. The head in metres was determined using calibration equations developed for each of the capacitance rods. The head (in metres) was then converted into discharge (Q) in litres/second (l/s) using the following formula (Evans and Riley, 1993):

$$Q = 18.4h \times 940h^2.$$

Each ripped plot had several raingauges throughout the site, and seven rainfall intensities were simulated for each ripped plot. Using the rainfall recorded in each raingauge on the ripped plot, I produced isohyets for each rainfall simulation, or "run". The isohyets for ripped plots 1 to 6, runs 1 to 7 are contained in Appendix D.

The average rainfall in each subplot was estimated from the isohyets. The subplot borders were overlayed on each isohyet graph and the average rainfall determined by adding the minimum rainfall and the maximum rainfall in each subplot and dividing by two. The results of these calculations are contained in Appendix C.

I calculated the rainfall weighting for each subplot and each run. The rainfall weighting was calculated from the following equation:

$$\text{Rainfall weighting} = \frac{\text{average rainfall for each subplot for each run}}{\text{Tipping Bucket raingage value for each run}}$$

The rainfall weighting's are contained in Appendix C.

## 2.4 Production of DISTFW NLFIT files

The DISTFW NLFIT model is a version of the Field Williams kinematic wave model that has been interfaced with the NLFIT package. The model and its application to waste rock dumps has been described in detail by Willgoose and Riley (1993), Finnegan (1993), Arkinstal *et al* (1994), and Evans, Riley, and Willgoose (1995).

NLFIT was developed by Kuczera (1994), and uses non-linear regression analysis to make parameter inferences based upon the available data and the predictive model being used.

The predictive model, the Field Williams kinematic wave model, was developed by Field and Williams (1985, 1987). This hydrology model includes the following features.

1. Non-linear storage of water on hillslope surfaces,
2. Discharge from groundwater storage to the channel,
3. Discharge from surface storage to the channel (overland flow), and
4. Routing of runoff in the channel using the kinematic wave.

The effect of groundwater on the Waste Rock Dump was assumed to be negligible for all DISTFW NLFIT model calibrations in this report.

The parameters used in the DISTFW - NLFIT Rainfall - Runoff model are described below.

- **Conveyance Parameters : $c_r$ , $e_m$**

$$K = c_r.A_r^{e_m}$$

The kinematic wave routing parameters are the components of the DISTFW model that most influences the scale dependent properties of the runoff hydrograph. Willgoose, Kuczera (1995) recommend that for natural hillslopes, $e_m$ ranges from 1.2 to 1.7.

The surface roughness, amount of rilling and undulations of the surface all influence the kinematic wave parameters.

- **Surface supply Parameters: $c_s$ and $\gamma$**

The surface supply parameters are negatively correlated. That is, as $c_s$ increases, $\gamma$ decreases. Increasing $c_s$ delays the arrival of the runoff to the mainstream of the catchment. If $c_r$ is fitted, $c_s$ is not altered, and vice versa.

- **Infiltration parameters: $S_\phi$ and $\phi$**

The infiltration parameters determine the volume of water that becomes quickflow. The continuing loss rate parameter, $\phi$, describes the infiltration rate when the soil is wet. Sorptivity, $S_\phi$, is the initial dryness of the soil. The continuing loss rate should vary little from storm to storm. Sorptivity varies according to rainfall history.

- **Subsurface Parameter: $c_g$**

The subsurface parameter determines the dynamics of subsurface flow. Increasing the subsurface parameter decreases the peak flow from the subsurface store and delays its arrival at the mainstream. For all nlfit files, the subsurface parameter was set at 1000. This was due to negligible subsurface flow on the waste rock dump.

The run type used to approximate the soil site in DISTFW is 'catchment'. The subcatchment characteristics (such as length, slope, area, etc.) have been estimated by Saynor *et al* (1995). The same subcatchment characteristics were used for the soil site calibration in this report.

The run type used to approximate the ripped plots in DISTFW is 'plot'. This run type divides a plot into a number of subplots. The upstream subplot drains into the downstream subplot and finally into a reservoir. Each subplot is assumed to have an equal width.

A Field-Williams input file was produced for runs 1,2,3 and 4 (group a) and a second Field-Williams file was produced for runs 4,5,6 and 7(group b) in each ripped plot.

The overlap of run 4 in each Field-Williams file was aimed to produce a set of parameters that would be similar for both run group 'a' and run group 'b' and for the entire set of runs on each ripped plot.

Rainfall and Runoff files were produced for four natural storm events on the soil site during the 95/96 wet season, and for each rainfall simulation on each ripped plot.

Times were adjusted to start at zero decimal hours and the discharge was converted to cubic metres per second for the runoff data file. The rainfall (in millimetres) and corresponding time (in decimal hours) were prepared for the rainfall data file.

Examples of rainfall, runoff and Field Williams files for the soil site are shown in Appendix E.

## 2.5 DISTFW NLFIT Calibration

The DISTFW NLFIT model was calibrated to determine catchment parameters for both the soil site and the ripped plots. The model achieves this by fitting a predicted discharge curve to an observed discharge curve. The parameters derived from DISTFW NLFIT for both the soil site and the ripped plots will be used to compare each site, and each rainfall event.

I calibrated DISTFW NLFIT for both the soil site and the ripped plots in the following steps:

1. Fit $C_r$ and $\phi$,

where, $C_r$ = channel conveyance coefficient

$\phi$ = long term steady state infiltration parameter.

This approximately fits the timing and the volume of the hydrograph (Willgoose, Kuczera, Williams, 1995).

2. Fit $S_\phi$ and $\phi$ (the infiltration parameters),

where, $S_\phi$ = initial dryness (sorptivity).

This step improves the fit of the volume of the hydrograph.

3. Fit $C_r$ and $e_m$ (conveyance parameters),

where, $e_m$ = the exponent on the kinematic wave equation.

This will fit the routing behaviour of the hydrograph more precisely.

4. All parameters used ($C_r$, $e_m$, $S_\phi$,$\phi$) were fitted simultaneously. This polished up the fit obtained in the previous steps.

After the above steps had been completed, a posterior moments file (.pmf) and a print file (.prt) were generated.

The group 'a' results were compared with the group 'b' results for each ripped plot using COMPAT. All six ripped plots, and all four rainfall events on the soil site were compared using COMPAT to determine whether there was any similarity. Graphs of $S_\phi$ versus $\phi$, and $C_r$ versus $e_m$ were produced.

Field-Williams model parameters were obtained using NLFIT. Version 2.07g. Initial parameter values were set at:

$C_r = 10$

$e_m = 1.67$

$C_s = 0.003$

$\gamma = 0.375$

$S_\phi = 0.001$

$\phi = 0.001$

$C_g = 1000$

Initial V #1 = 0

Initial V #2 = 0

Initial V #3 = 0

Initial V #4 = 100.

# 3. ANALYSIS AND CALIBRATION

## 3.1 95/96 Wet Season Soil Site Hydrology

Discharge hydrographs for both the observed and logged events are given in Appendix F. An example of an observed discharge hydrograph is shown in Figure 4 below for the rainfall event monitored on the 10th January 1996.

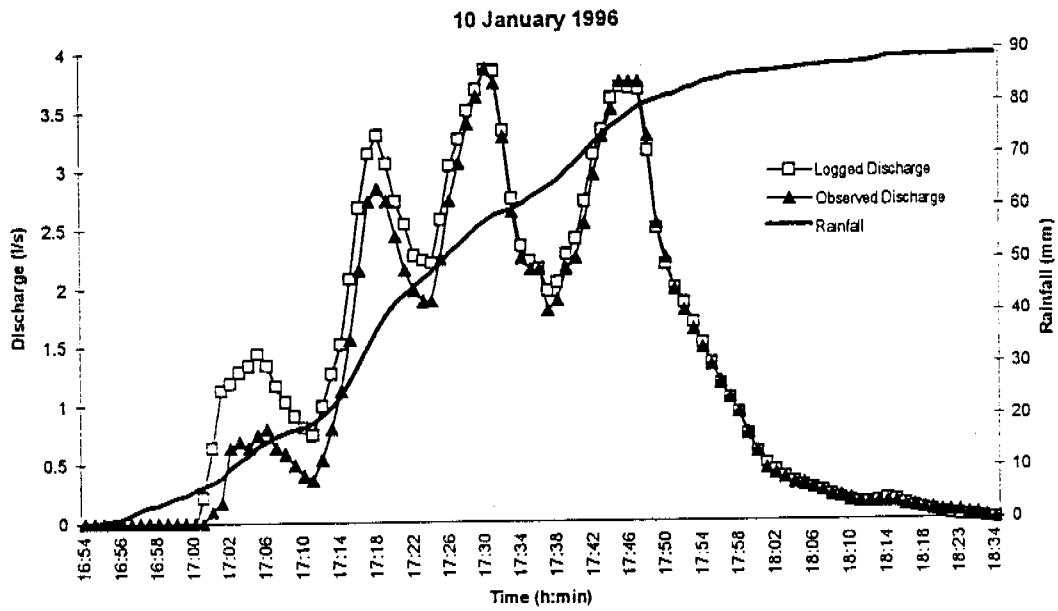


Figure 4 - Observed rainfall event on 10th January 1996

The capacitance rod, used to measure the depth of water over the flume, varies with temperature. Errors associated with this resulted in some of the logged storms having negative discharges. The storms showing negative discharges in the Appendix F hydrographs were not used in the DISTFW NLFIT model.

Figure 5 below shows the cumulative rainfall and total runoff for each storm monitored throughout the 95/96 wet season.

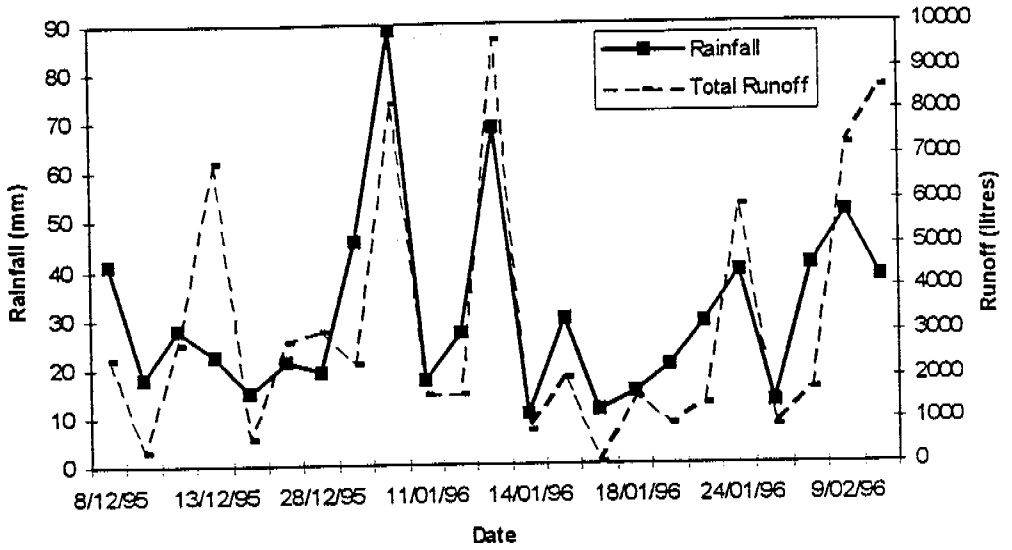


Figure 5 - Rainfall and Runoff events monitored during 95/96 Wet Season

Log relationships between Rainfall and Runoff are given in Figures 6a and 6b below.

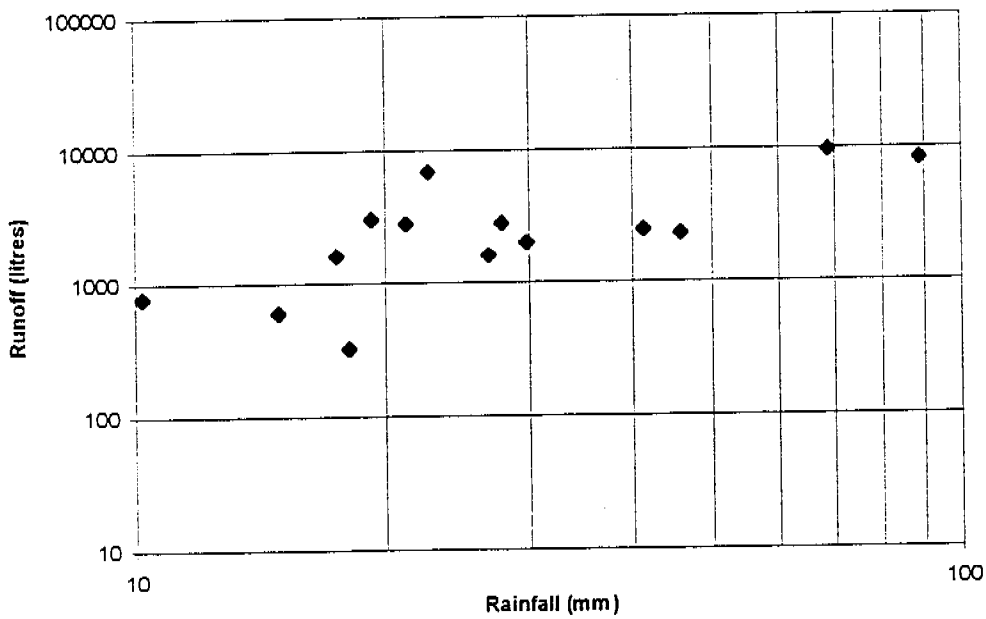


Figure 6a - Log Rainfall Vs Log Runoff between 14/12/95 and 16/1/96

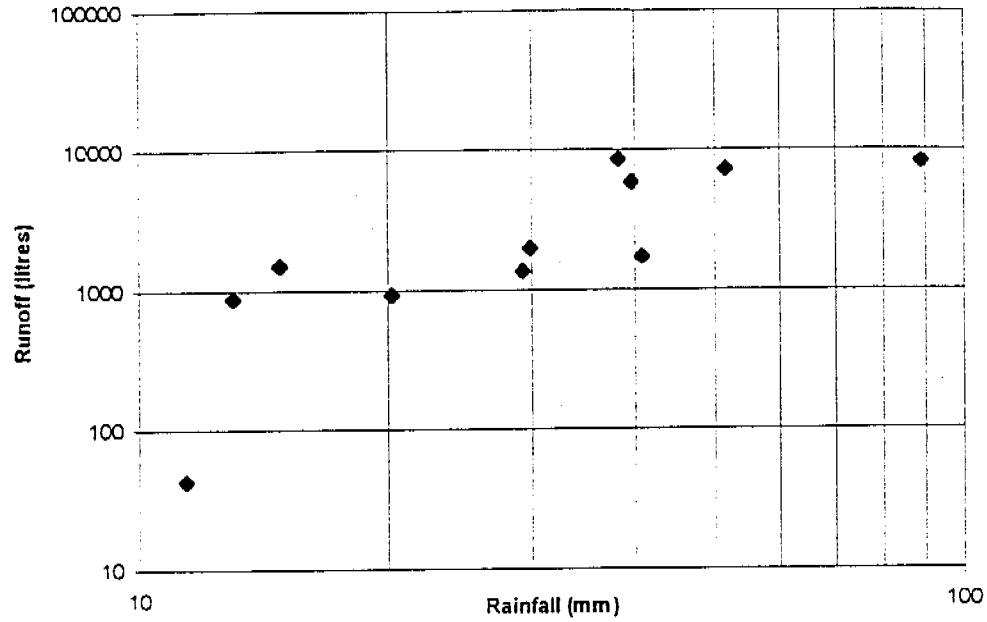


Figure 6b - Log Rainfall Vs Log Runoff between 16/1/96 and 10/2/96

Dividing the storms into the beginning and end of the wet season, and plotting the log rainfall against log discharge shows that the slope between the two graphs (beginning and end) does not vary significantly. This indicates that the vegetation growth between the beginning and end of the wet season does not have a significant effect on the runoff from the soil site.

The rainfall intensity was compared with the steady infiltration rate for four storms over the 95/96 wet season, as shown in Figure 7 below

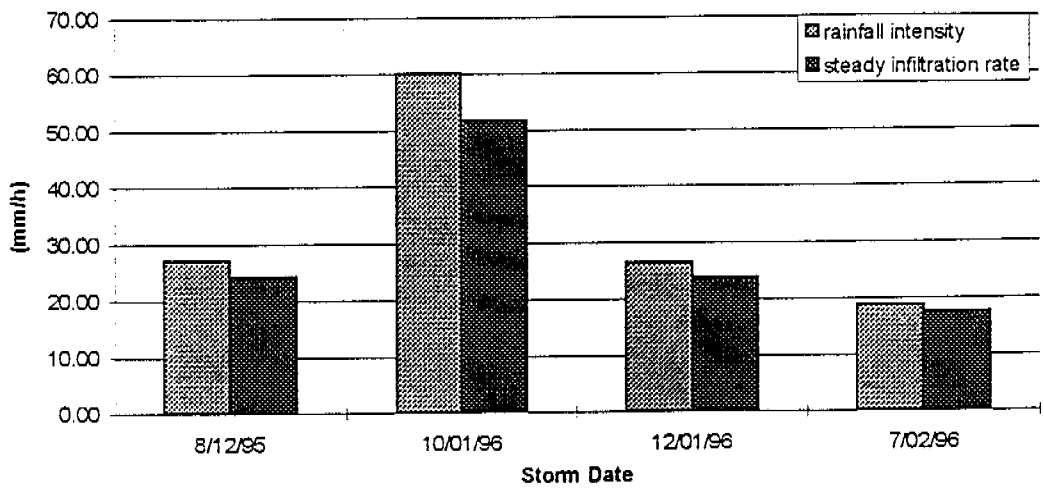


Figure 7 - Rainfall intensity and steady infiltration rate

The steady infiltration rate was calculated by subtracting the net rainfall rate from the rainfall intensity. The net rainfall rate is the depth of rainfall on the surface divided by the storm duration. The depth of rainfall on the surface is the volume of rainfall leaving the site divided by the area of the soil site (600 $m^2$).

Figure 7 shows the infiltration on the soil site is extremely high. The difference between the rainfall intensity and the steady infiltration rate is the runoff from the site. Figure 7 shows the runoff from the soil site is minimal.

DISTFW NLFIT was calibrated for the following four storms; 8/12/95, 10/1/96, 12/1/96 and 7/2/96. The NLFIT graphs for the four storms are contained in Appendix G. The parameters calibrated for the above storms are found in Table 2 below.

Table 2 - Soil Site parameter values

| Parameter | 8/12/95 | 10/1/96 | 12/1/96 | 7/2/96 |
|---|---|---|---|---|
| $c_r$ | 0.245 | 0.575 | 1.285 | 9.016 |
| $e_m$ | 0.933 | 1.088 | 1.212 | 1.881 |
| $S_\phi$ | 0.001 | 0.543 | 0.001 | 4.200 |
| $\phi$ | 70.537 | 41.895 | 48.320 | 52.916 |

COMPAT was used to assess the similarity between the four storms on the soil site. The COMPAT graphs are shown in Figures 8a and 8b below.

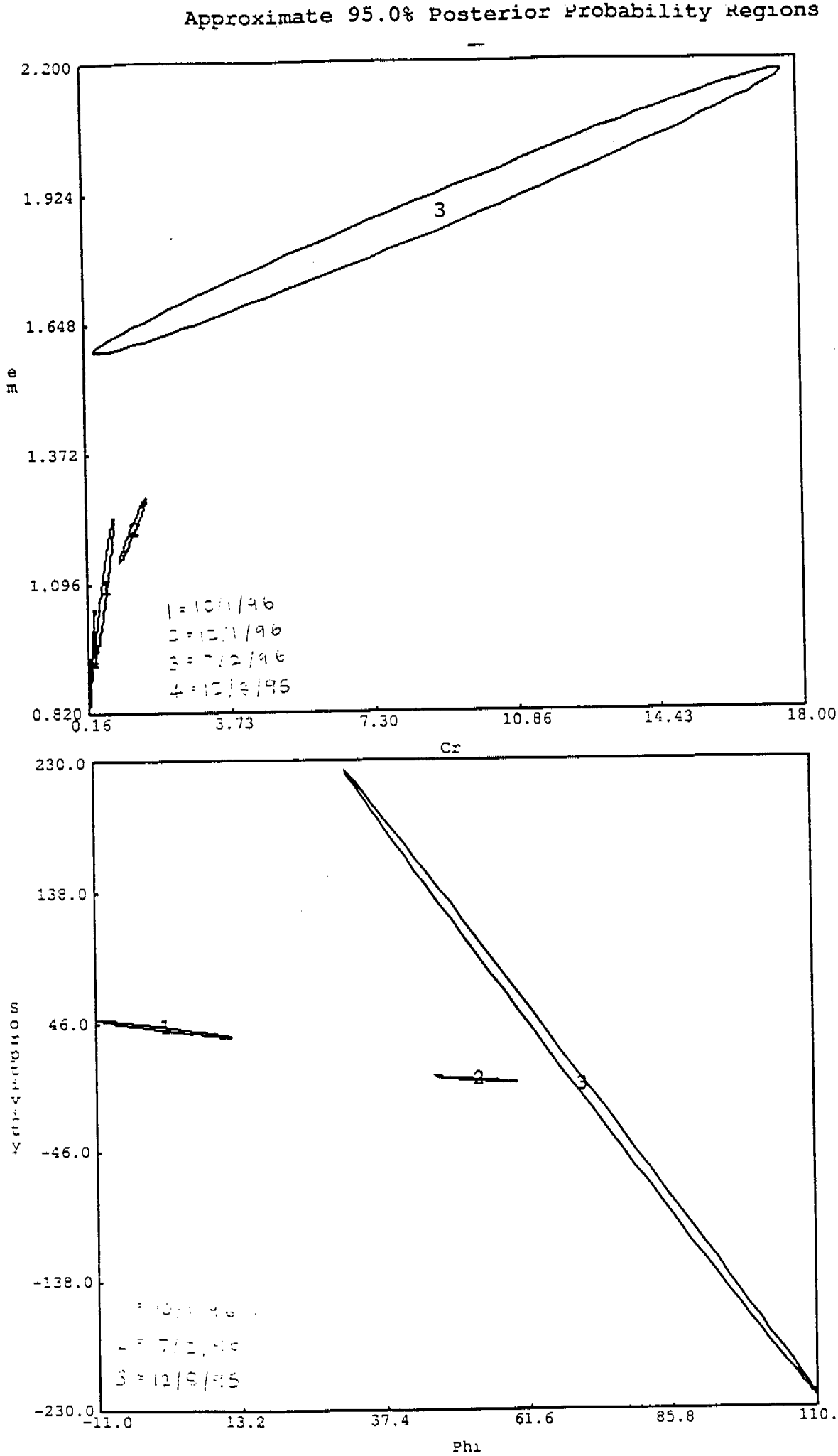


Figures 8a and 8b - COMPAT graphs of soil site storms fitted with different parameters

The graphs of Figures 8a and 8b show that there is some variation with the parameters fitted for the four storms over the 95/96 wet season.

The four storms on the soil site were also fitted for one set of parameters. The NLFIT graphs resulting from this fit are contained in Appendix G. The calibrated parameters for the four storms fitted together are shown in Table 3 below.

Table 3 - Calibrated parameters for all four storms on soil site

| Parameter | Mean |
|---|---|
| $c_r$ | 0.203 |
| $e_m$ | 0.980 |
| $S_\phi$ | 0.001 |
| $\phi$ | 74.460 |

The similarities between each storm event calibrated using the above set of parameters is shown with the COMPAT graphs in Figures 9a and 9b below.

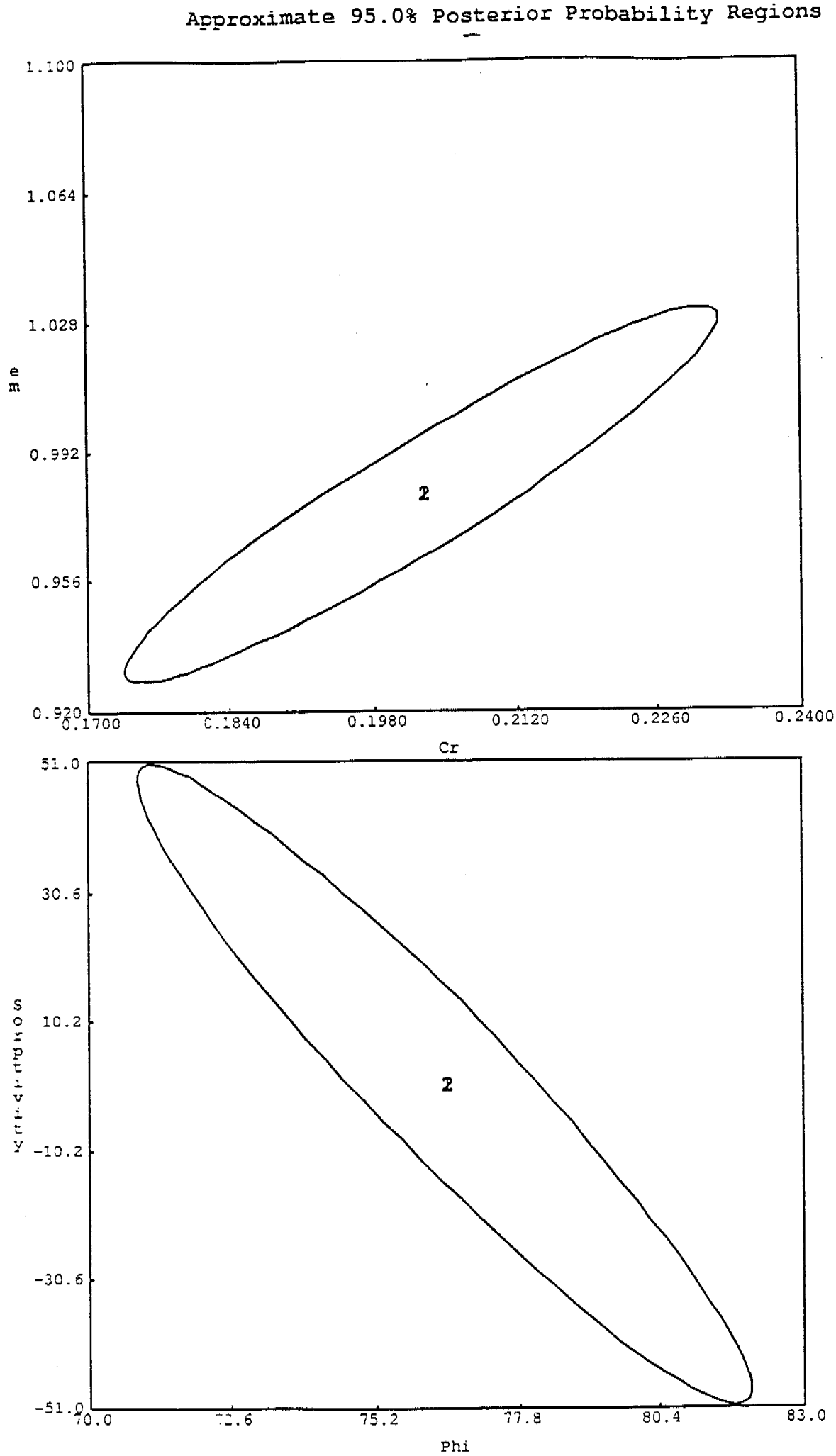


Figures 9a and 9b - COMPAT plots of soil site storms fitted with one set of parameters

## 3.2 1993 Ripped Plot Hydrology

The observed and predicted discharge versus time series, normal probability, COMPAT plots, and tables showing the fitted parameters are contained in Appendix H.

Table 4 below summarises the fitted parameters between group 'a' and group 'b' for all ripped plots using the 1993 simulations.

Table 4 - Fitted parameters for all Ripped Plots

| Parameter | Ripped Plot | | | | | |
|---|---|---|---|---|---|---|
| | 1 | 2 | 3 | 4 | 5 | 6 |
| $c_r$ | 1.141 | 20.13 | 15.029 | 1.7411 | 21.3 | 18.179 |
| $e_m$ | 1.1607 | 1.8298 | 2.0297 | 1.4485 | 2.0955 | 1.6186 |
| $S_\phi$ | 4.0704 | 0.2385 | 0.001 | 0.001 | 0.001 | 0.0623 |
| $\phi$ | 73.984 | 11.807 | 68.134 | 15.852 | 187.54 | 96.815 |

The similarities between the six ripped plots were compared using 'compat'. The compat graphs are shown in Figures 10a and 10b.

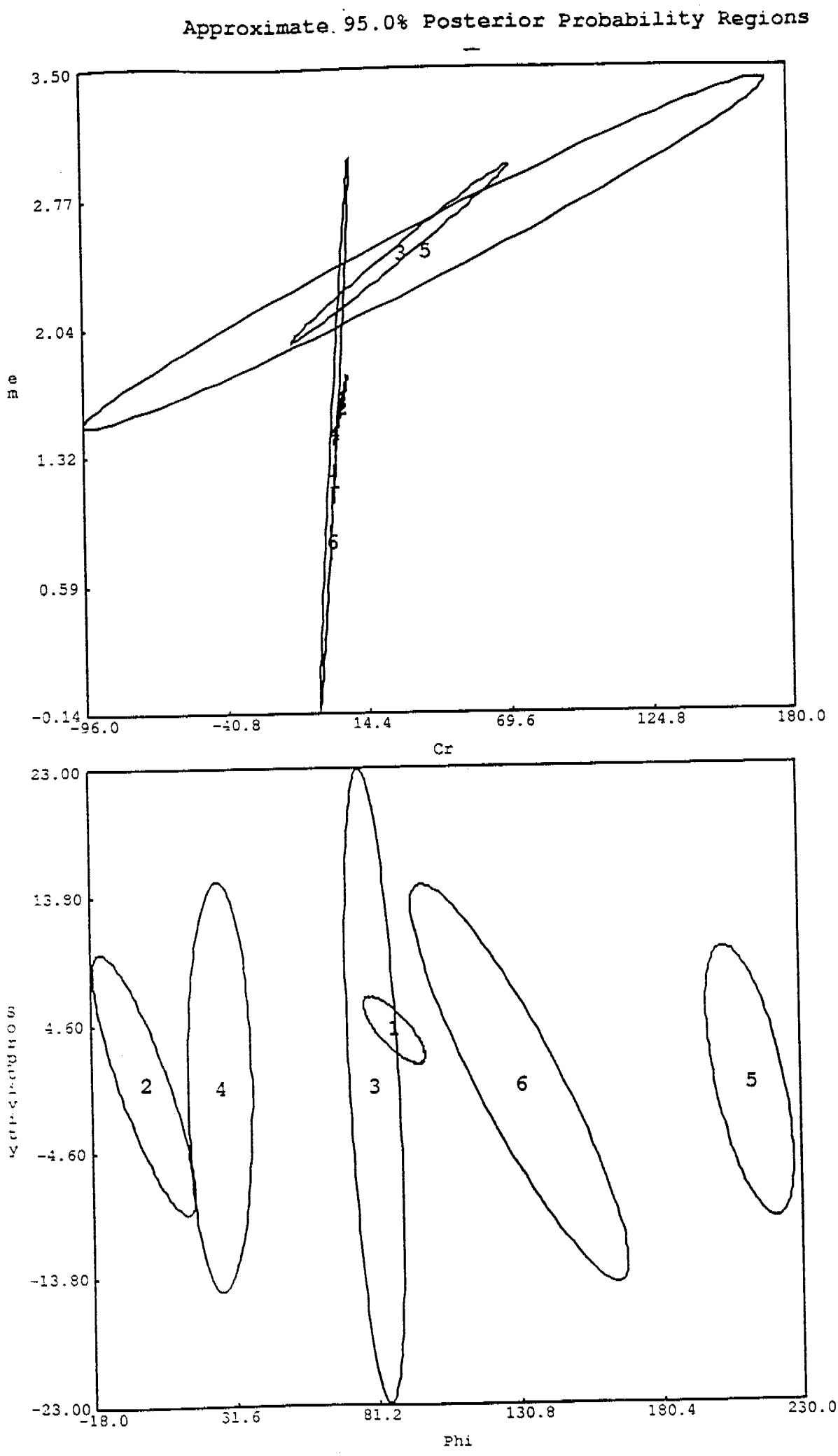


Figures 10a and 10b - COMPAT graphs of six ripped plots

The graphs in Figures 10a and 10b show that the 95% probability regions were similar for all six plots for the kinematic wave parameters $c_r$ and $e_m$ .This indicates that all six ripped plots have similar kinematic wave properties (similar surface roughness, amount of rilling and undulations). The compat plot of $S_\phi$ and $\phi$ indicate that all six ripped plots have similar sorptivity (similar rainfall history), but a varying long term infiltration rate.

The ripped plots with similar ripping strategies to the soil site were plots 3, 4, and 5. These plots were calibrated together to determine the common parameter values and are summarised in Table 5 below.

Table 5 - Calibrated parameters for Ripped Plots 3, 4, and 5

| Parameter | Mean |
|---|---|
| $c_r$ | 1.8662 |
| $e_m$ | 1.5846 |
| $S_\phi$ | 0.001 |
| $\phi$ | 40.358 |

The DISTFW NLFIT graphs for ripped plots 3, 4, and 5 fitted with the above parameters are contained in Appendix H. The COMPAT plots comparing the 95% posterior probability regions of the three ripped plots are shown in Figures 11a and 11b below. The large probability regions indicate that the errors associated with the three ripped plots are large.

The graphs of Figures 11a and 11b show that the 95% posterior probability region for the parameters fitting the ripped plots 3, 4, and 5 are much larger than the region for Figures 9a and 9b, the COMPAT graphs of the four soil site storms.

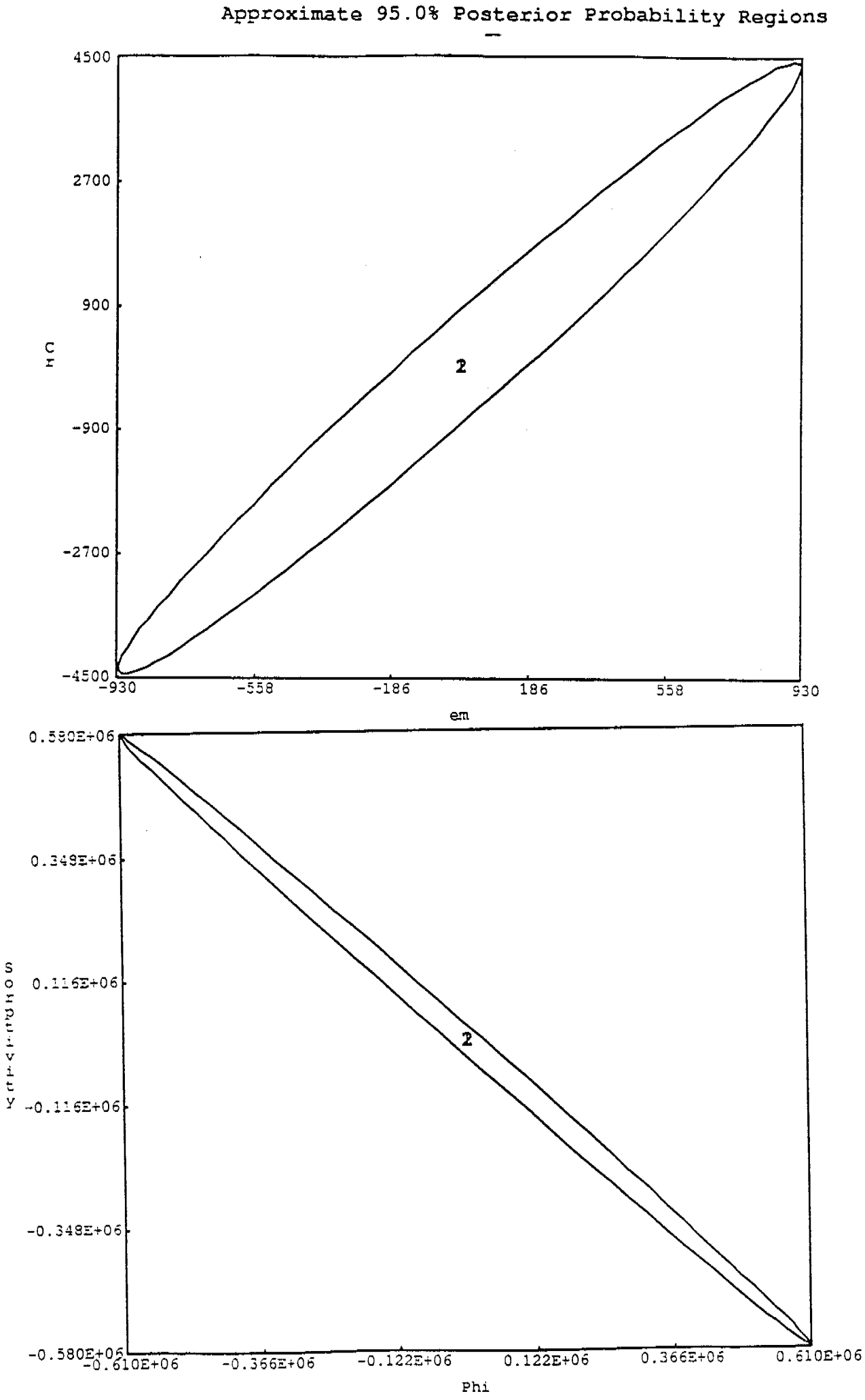


Figures 11a and 11b - COMPAT graphs of Ripped Plots 3, 4, and 5

## 3.3 95/96 Wet Season Soil Site Sediment

Copies of the bedload sample analysis and suspended sediment files are contained in Appendix I.

Figure 12 gives the bedload eroded from the site with each monitored storm in the 95/96 wet season.

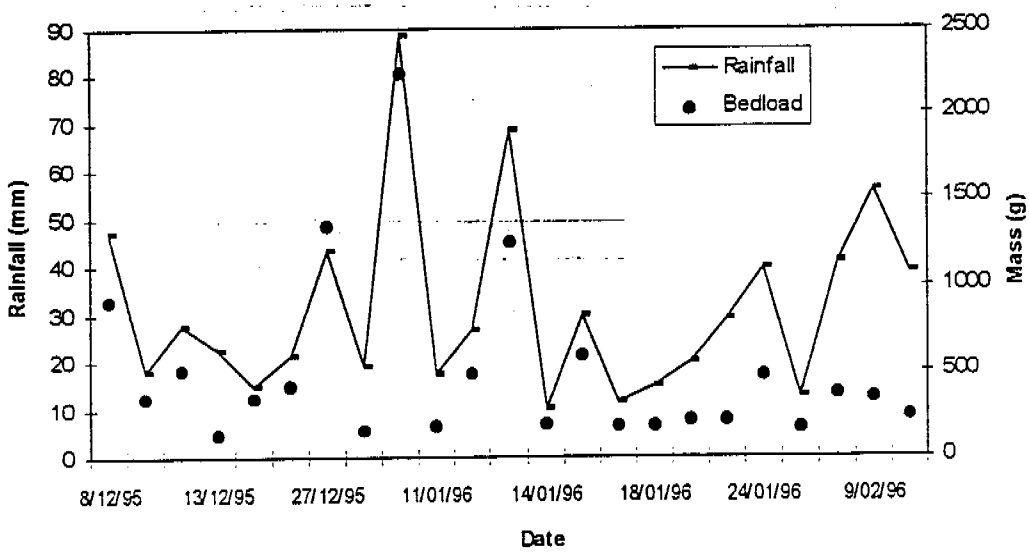


Figure 12 - Bedload and Rainfall Events monitored during 95/96 Wet Season

Log graphs between bedload and rainfall shown in Figures 13a and 13b below.

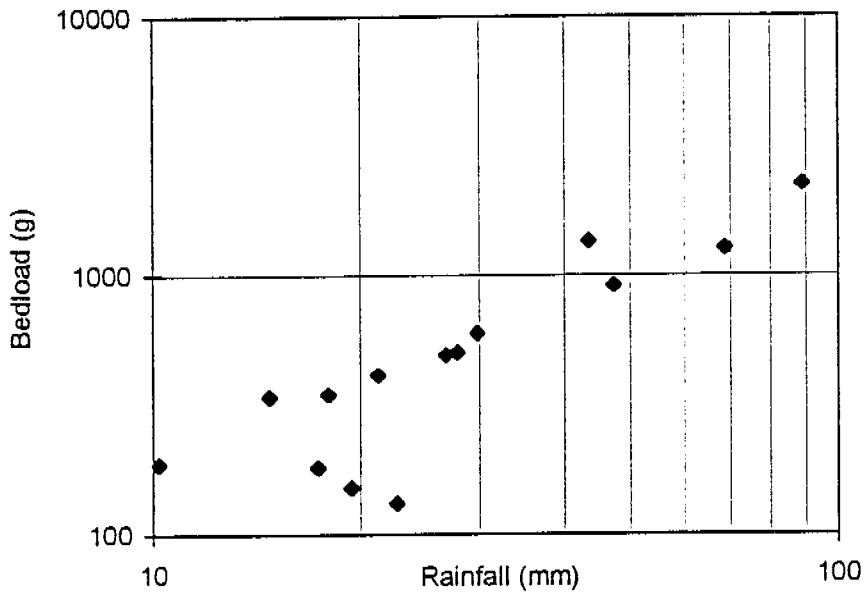


Figure 13a - Log Rainfall Vs Log Bedload for storms between 8/12/95 and 16/1/96

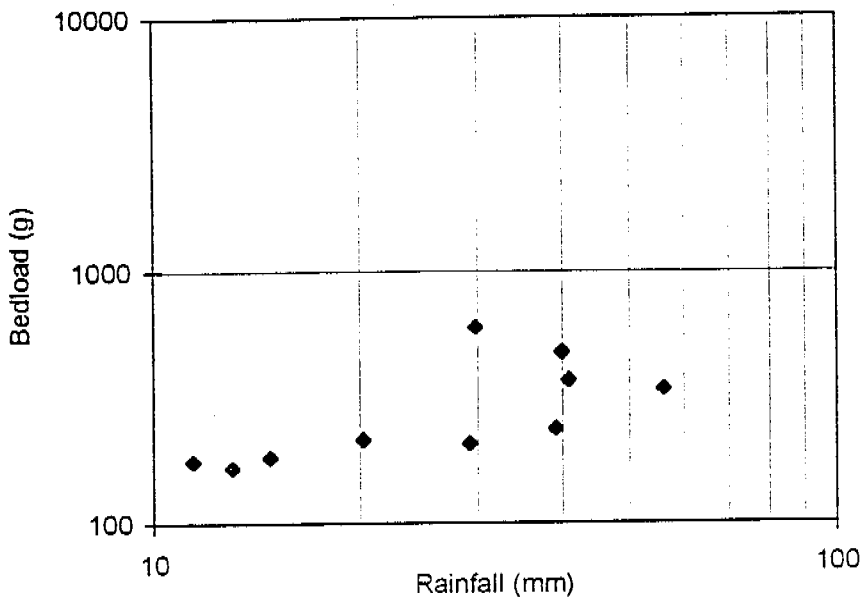


Figure 13b - Log Rainfall Vs Log Bedload for storms between 16/1/96 and 10/2/96

The slope of log bedload against log rainfall does vary between the beginning and end of the wet season. This indicates that the vegetation does have an effect on the erosion of the soil site.

The variation in particle size throughout the wet season is shown in Figure 14 below. The horizontal axis shows the fraction of total bedload sample that was collected in each particular sieve size. There is no trend in the variation of particle size throughout the season.

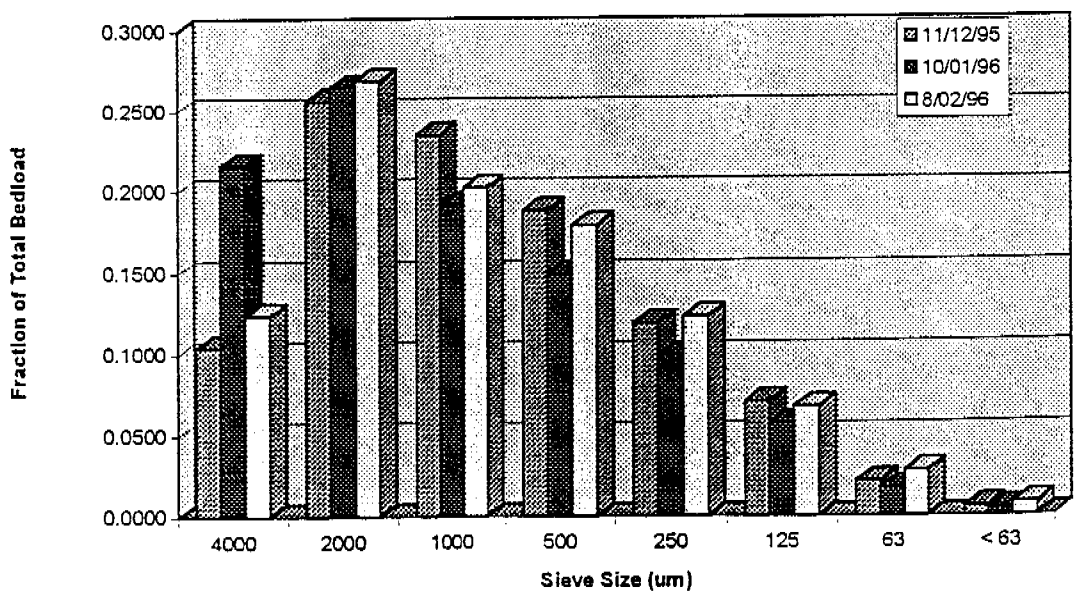


Figure 14 - Variation in Bedload Particle size throughout 95/96 Wet Season

Suspended Sediment was analysed for the observed storms on 14/12/95 and 10/1/96. The variation of suspended sediment concentration with discharge throughout each observed storm event is shown in Appendix J. The Sediment Transport Equation can be used to model these graphs. The sediment transport equation described in Willgoose and Riley (1993) is given below.

$$q_s = \beta . q^m . S^n$$

Where, $q_s$ = sediment discharge/unit width ($g\ s^{-1}\ m^{-1}$);

q = discharge/unit width ($ls^{-1}\ m^{-1}$);

S = local slope (m/m); and

$\beta$, m, and n are parameters fixed by flow geometry and erosion physics.

The log of sediment against log of discharge approximates a straight line. This supports the sediment transport equation above (due to $\log q_s = \log \beta + (m-1)\log q$ for a constant slope).

## 3.4 95/96 Wet Season Soil Site Vegetation

Photographs showing the growth of vegetation throughout the 95/96 wet season are contained in Appendix A. Photographs of the $1m^2$ quadrats used to estimate the percentage cover are also contained in Appendix A.

Figure 15 below shows the variation in percentage cover, biomass, and average grass height throughout the wet season.

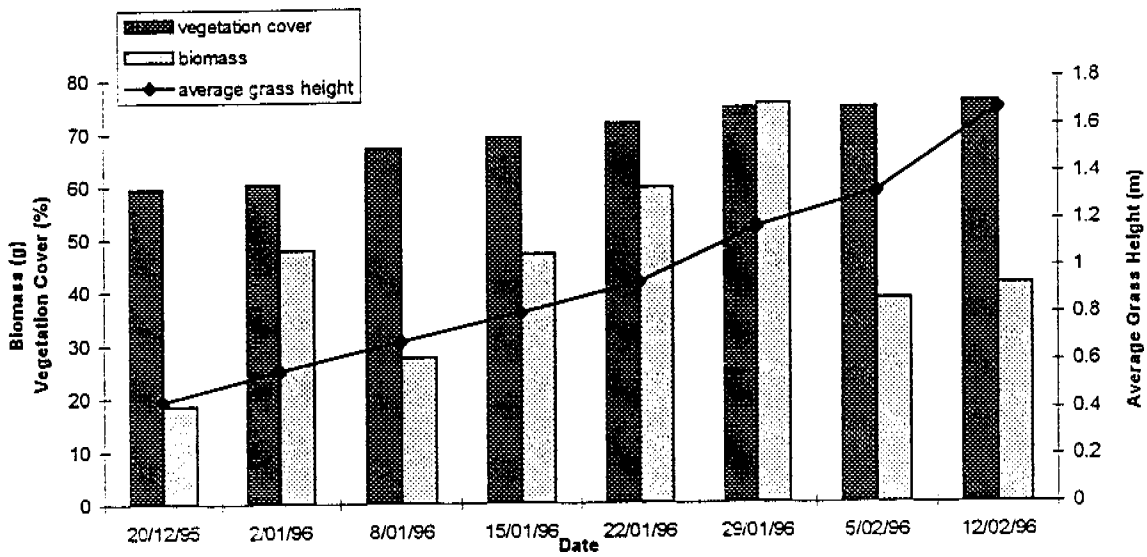


Figure 15 - Variation in percentage cover, biomass, and average grass height over wet season

The average grass height increases as the wet season proceeds. Neither the percentage vegetation cover or the biomass on the soil site changes significantly.

The relationships between vegetation cover, biomass, and average grass height are shown in Figures 16a, 16b, and 16c below.

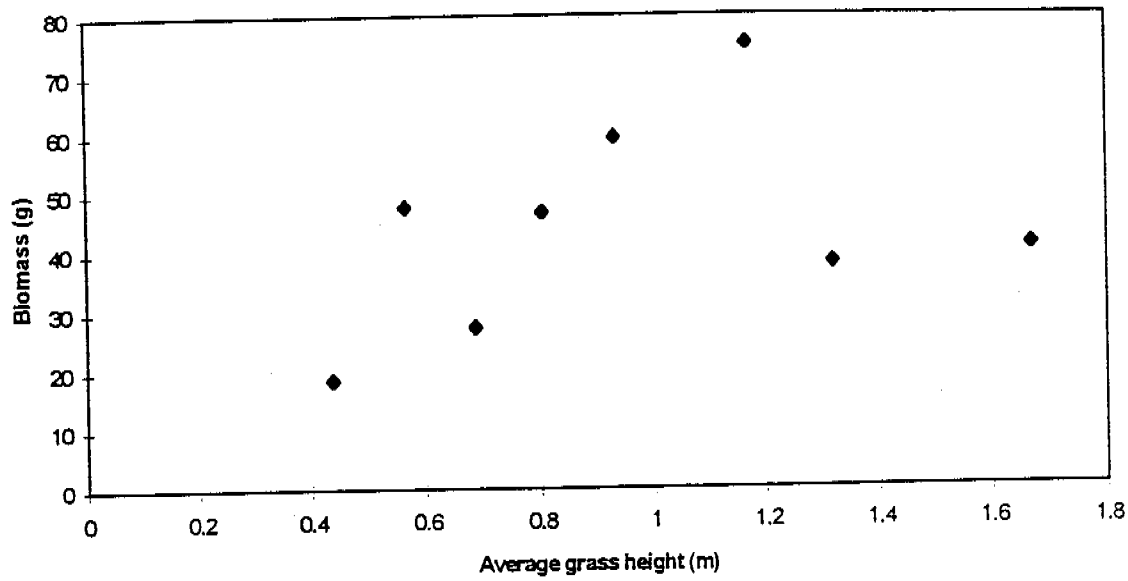


Figure 16a - Relationship between Biomass and Average grass height

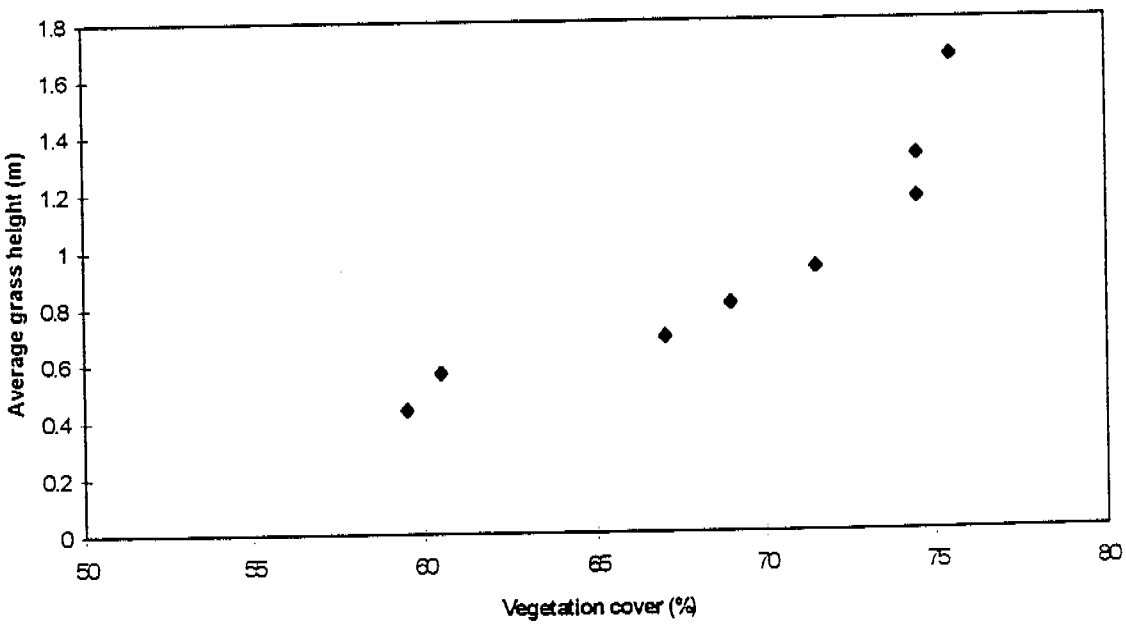


Figure 16b - Relationship between Average grass height and Vegetation cover

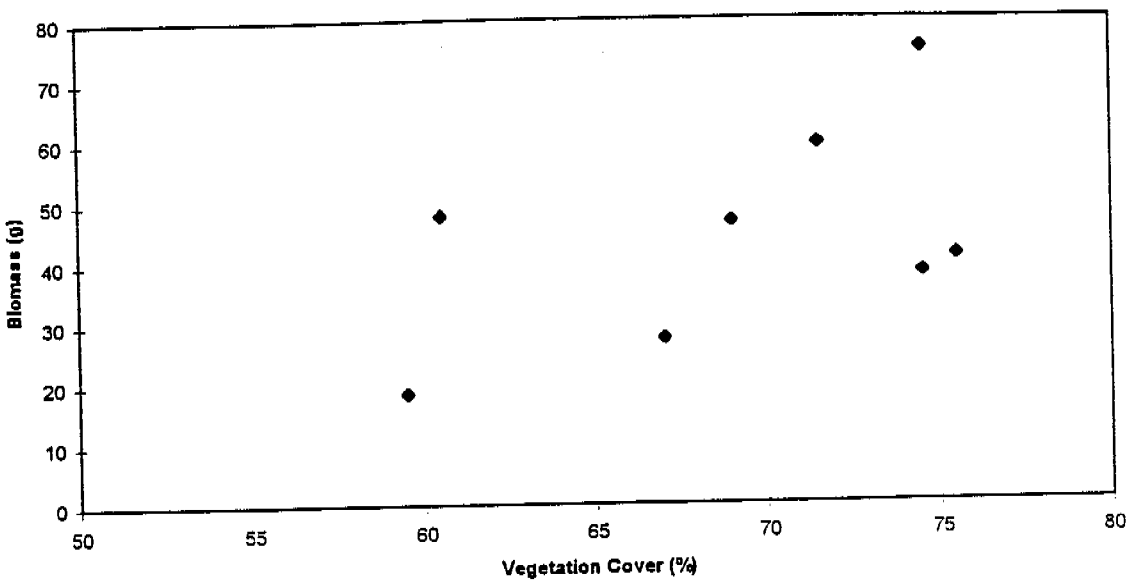


Figure 16c - Relationship between Biomass and Vegetation cover

The slope of the graph in Figure 16a shows that as the average grass height increases on the soil site, so does the biomass. Figure 16b shows the average grass height increases with the percentage vegetation cover. Figure 16c indicates as the percentage vegetation increases, so does the biomass.

Tabulated results for the vegetation are shown in Appendix K.

# 4. DISCUSSION

## 4.1 Effect of Vegetation on Hydrology

Figures 6a and 6b show that the slope of the graphs between the beginning and end of the wet season do not vary significantly. This indicates that the vegetation growth between the beginning and end of the wet season does not have a significant effect on the runoff from the soil site.

Figure 7 shows the infiltration on the soil site is extremely high and the runoff from the soil site is minimal. Finnegan (1993) also found high infiltration rates. It is unknown whether the high infiltration rates are due to the vegetation. There is not a constant increase in infiltration over the wet season.

The DISTFW NLFIT model prediction of the parameter values for the soil site in Table 2 show that as the wet season proceeds from 8th December 1995 to 7th February 1996, the kinematic wave parameters increase. The increase in kinematic wave parameters result in an increase in discharge off the site. This may be due to the rips being worn down and eroded away.

For all four storms fitted on the soil site, the long term infiltration parameter was large. This supports Figure 7. The infiltration parameters did not vary significantly throughout the wet season. From recent consultation with Ken Evans, at ***eriss***, rainfall simulations carried out on the soil site before and after burning also show no significant change in the infiltration parameters.

The root network of spear grass that is just under the surface at the beginning of the wet season may reduce the runoff from the soil site. The ability of the roots to hold the soil and waste rock together may exist in the ground throughout the entire year. The time between the grass dying off (or being burnt) should not be long enough for the roots to degrade and loose their reinforcing ability as the vegetation on the soil site is well established.

## 4.2 Effect of Ripping on Hydrology

### 4.2.1 Effect of Ripping Pattern (1993)

Figures 11a and 11b show that the errors associated with ripped plots 3, 4, and 5, after they were calibrated together, are large. This may be due to the different characteristics of each ripped plot, or inconsistencies in the 1993 ripped plot data, such as the spatial distribution of the rainfall with time.

### 4.2.2 Comparison between Ripped Plots and Soil Site

Ripped plots 3, 4, and 5 (refer to Figure 3) were found to have similar parameters to each other and to the soil site. Figure 17a and 17b below show the comparisons between the ripped plots 3, 4, and 5; and the soil site 95/96 wet season storms.

The 95% posterior probability region for the infiltration parameters, $S_\phi$ and $\phi$ shows that the variation for the ripped plot parameters are extremely large. The variation in the kinematic wave parameters, $c_r$ and $e_m$ are also extremely large for the ripped plots. Due to the large inconsistencies associated with the ripped plot parameters, the ripped plots cannot be compared to the soil site parameters. Thus, the effect of ripping cannot be disaggregated from the soil site, making the true effect of vegetation on the hydrology of the soil site unknown. It is believed the effect of ripping diminishes with time while the vegetation should be sustainable.

Additional data is required to determine the hydrology of an unvegetated site. This site must have no underlying root network and a similar ripping pattern to the soil site. Comparing this data with the soil site results would enable the effect of vegetation on the hydrology of the waste rock to be determined.

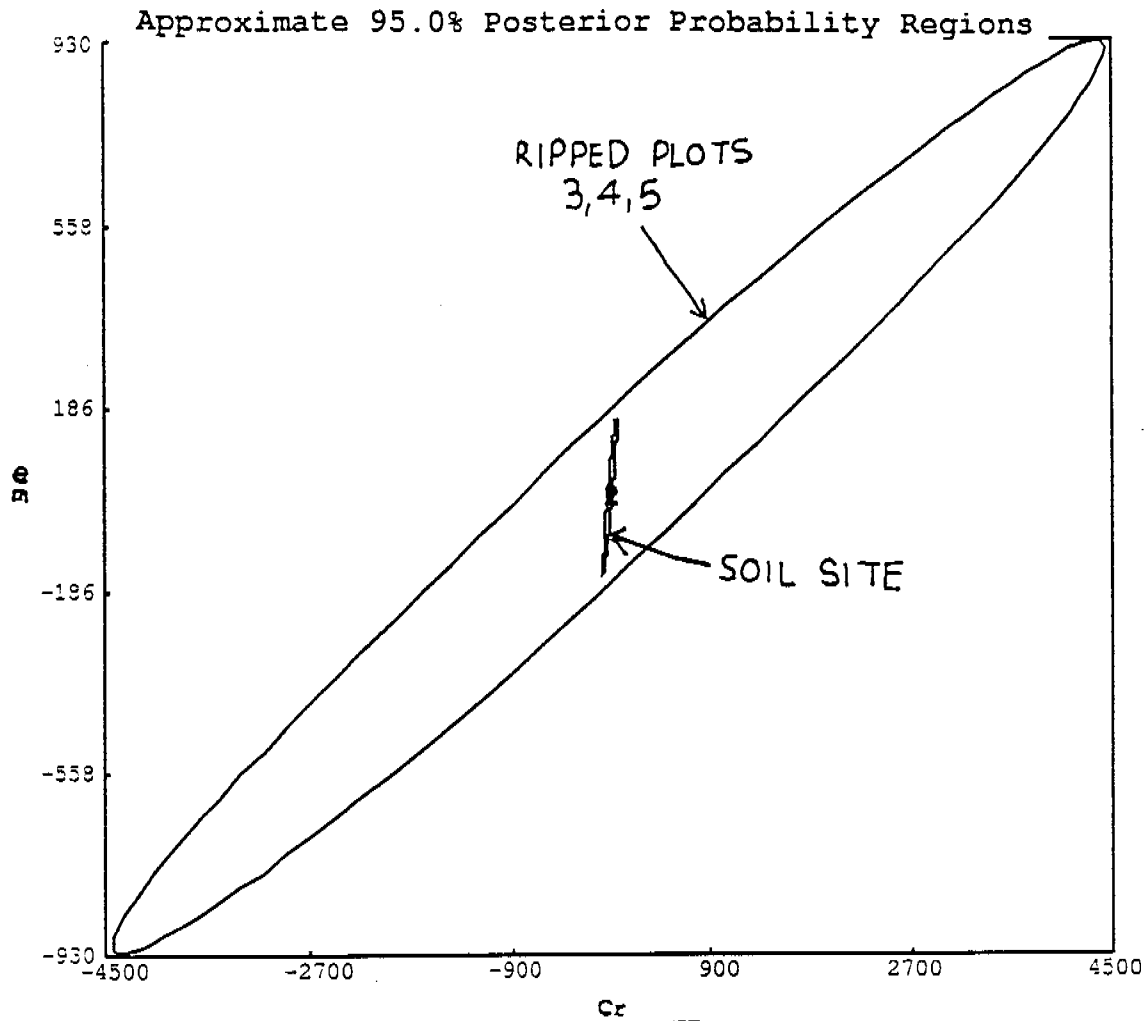


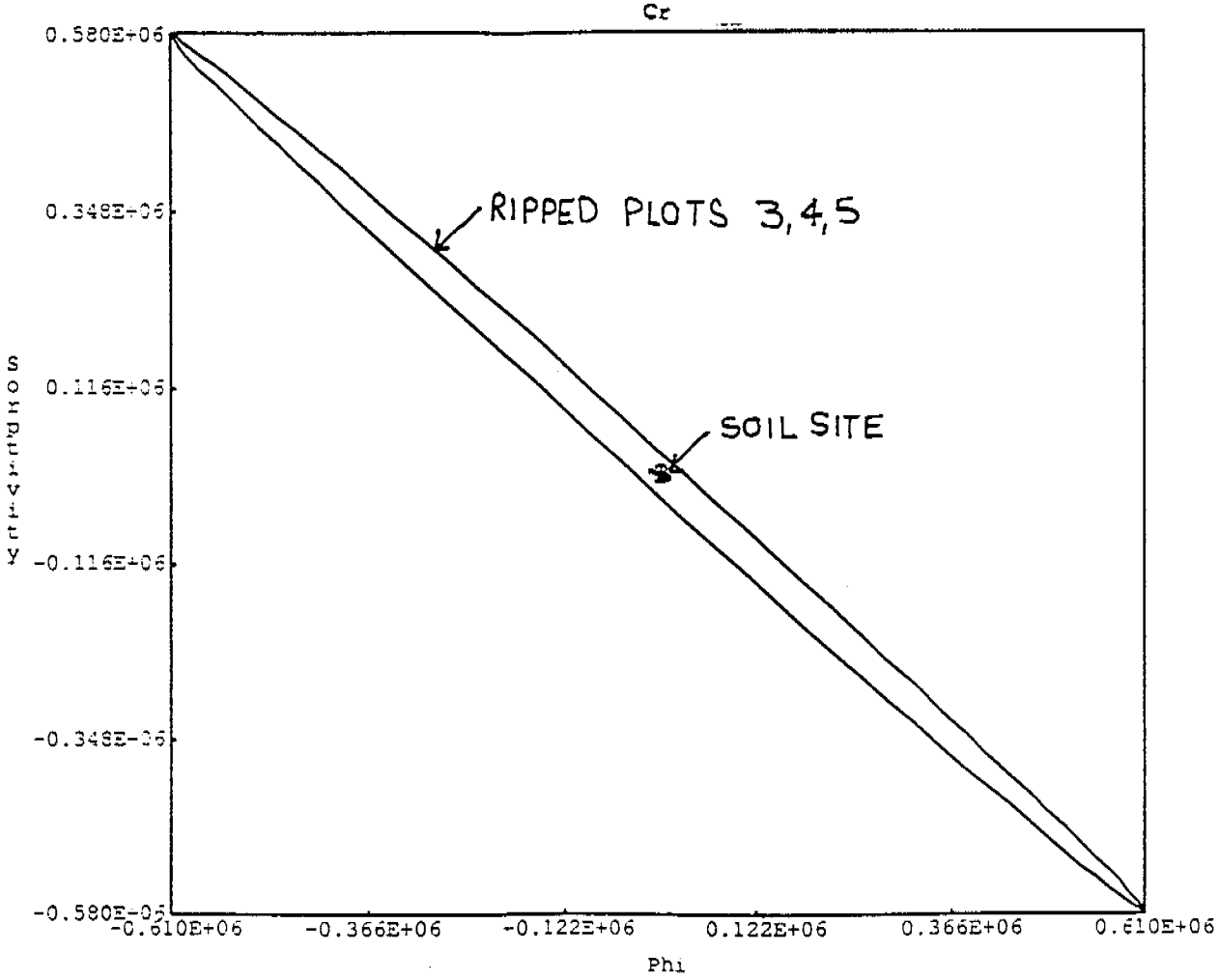


Figure 17a and 17b - COMPAT graphs of Ripped Plots and Soil Site

## 4.3 Effect of Vegetation on Erosion

Figure 13 shows the slope of log bedload against log rainfall does vary between the beginning and end of the wet season. This indicates that the vegetation does have an effect on the erosion of the soil site. As the wet season proceeds, the amount of erosion off the soil site for a particular rainfall event is decreased.

# 5. CONCLUSIONS

The vegetation was found to have no significant effect on the hydrology of the soil site between the beginning and end of the wet season.

The soil site has extremely high infiltration rates. These rates do not change significantly as the wet season proceeds.

Erosion on the soil site was found to decrease as the 95/96 wet season proceeded.

The comparisons between the six ripped plots show that there is no significant difference between the different ripping strategies with regard to the infiltration and kinematic wave parameters.

The effect of vegetation on the hydrology of the soil site cannot be accurately assessed by comparing it with the 1993 Ripped Plot data due to the inconsistencies in the Ripped Plot data.

# 6. ACKNOWLEDGMENTS

Thanks are expressed to all those people who gave their time and expertise to assist with this project. Without such guidance and support, the extent of work that was able to be achieved would not have been of the same quality or magnitude.

In particular I would like to thank the following people:

Dr Garry Willgoose my supervisor at The University of Newcastle and Mr Ken Evans my supervisor at ***eriss***. Dr George Kuczera for his advice with NLFIT.

Mr M Saynor (***eriss***) and Mr B Smith (***eriss***) who assisted with the wet season monitoring, laboratory and data analysis. Mr T House (***eriss***) for his assistance with computer applications.

The ripped plot study was developed by Dr S Riley while at ***eriss***.

# 7. REFERENCES


Arkenstal, M., Willgoose, G.R., G.R., Loch, R.J. and Pocknee, C. 1994. *Calibration of DISTFW parameters for the QDPI rainfall simulator Oaky Creek,* Research Report No. 093.04.1994, The University of Newcastle, Department of Civil Engineering and Surveying.

Commonwealth of Australia. Department of the Arts, Sport, the Environment, Tourism and Territories. 1987. *Code of Practice on the management of radioactive waste from the mining and milling of radioactive ores 1982. Guidelines.* AGPS, Canberra.

Evans KG, Saynor, M.J., Willgoose GR. 1996. The effect of vegetation on waste rock erosion, Ranger Uranium Mine, Northern Territory. *The AusIMM Bulletin,* **No. 6** September, pp 21-24.

Evans KG, Riley SJ, Willgoose GR. 1995. Calibration of DISTFW rainfall-runoff model parameters using rainfall simulator data from the cap site at Ranger Uranium Mine NT: Preliminary Report. Internal Report 183, , Supervising Scientist for the Alligator Rivers Region, Canberra.

Evans KG & Riley SJ. 1993. Regression equations for the determination of discharge through RBC flumes. Internal report 104, Supervising Scientist for the Alligator Rivers Region, Canberra. Unpublished paper.

Field, W.G. and Williams, B.J. 1985. *A generalized kinematic catchment model.* Engineering Bulletin CE14. The University of Newcastle.

Field, W.G. and Williams, B.J. 1987. A generalised kinematic catchment model. *Water Resour. Res.* 23(8), pp 1693 - 1696.

Finnegan, L.G. 1993. Hydrologic characteristics of deep ripping under simulated rainfall at Ranger Uranium Mine. Commonwealth of Australia. Office of the Supervising Scientist internal report IR 134.

George, E.M. 1996. Ripped plot hydrology RUM 1993, and Wet season monitoring fire and soil sites, WRD, RUM 1995-96. Internal report IR 201, Supervising Scientist for the Alligator Rivers Region.

Kuczera, G. 1994. *NLFIT users manual,* Research Report, Department of Civil Engineering and Surveying, The University of Newcastle.

Kuczera, G. 1995. CIVL342 : Hydrology Lecture Notes. Department of Civil Engineering and Surveying, The University of Newcastle.

Philip, J.R. 1969. Theory of Infiltration, Advances in Hydrosciences, 5, 215 - 296.

Saynor, M.J., Evans K.G., Smith, B.L., Willgoose G.R., 1995. Experimental study on the effect of vegetation on erosion of the Ranger Uranium Mine Rock Waste Dump. Natural rainfall monitoring data 1994/95 Wet season. Erosion and hydrology model calibration. Internal report IR 195, Supervising Scientist for the Alligator Rivers Region.

Streeter, V.L. and Wylie, E.B. 1988. *Fluid Mechanics*. McGraw-Hill, Singapore.

Willgoose, G.R., Kuczera, G.A. 1995. Estimation of Subgrid Scale Kinematic Wave Parameters for Hillslopes. *Hydrological Processes.* **9**. pp 469 - 482.

Willgoose, G.R., Kuczera, G.A., and Williams B.J. 1995. *DISTFW-NLFIT: rainfall-runoff and erosion model calibration and model uncertainty assessment suite user manual,* Research Report No. 108.03.1995, The University of Newcastle, Department of Civil Engineering and Surveying.

Willgoose, G.R., Riley, S. 1993. The assessment of long-term erosional stability of engineered structures of a proposed mine rehabilitation, in *Environmental Management, Geo-Water & Engineering Aspects* (Eds. Chowdhury and Sivakumar) Rotterdam.

# APPENDICES

Appendix A. Photographs of the Soil Site during the 95/96 wet season

Appendix B. Contour Maps of Ripped Plots 1 to 6

Appendix C. Subplot properties and plot areas for Ripped Plots 1 to 6

Appendix D. Isohyets from 1993 rainfall simulations on Ripped Plots 1 to 6

Appendix E. Sample .fw, .ro, and .rf files for NLFIT calibration of Soil Site

Appendix F. Monitored and Logged storm hydrographs for Soil Site during 95/96 wet season

Appendix G. DISTFW NLFIT calibration plots for 95/96 wet season soil site data

Appendix H. DISTFW NLFIT calibration plots for 1993 Ripped Plot data, and tables containing fitted parameters and their standard deviations

Appendix I. Bedload and Suspended Sediment results for Soil Site during 95/96 wet season

Appendix J. Sediment graphs for Soil Site during 95/96 wet season

Appendix K. Vegetation results for Soil Site during 95/96 wet season